Face Image Conformance to ISO/ICAO Standards in Machine Readable Travel Documents

Matteo Ferrara, Annalisa Franco, Dario Maio, *Member, IEEE*, and Davide Maltoni, *Member, IEEE*

***Abstract*—Face images to be included into machine readable travel documents have to fulfill quality requirements defined by international ISO standards. The concept of quality in this context extends the common idea of image quality: usually a bad quality image presents visual defects such as blurring or noise while, according to ISO/ICAO standard, other factors could make a given sample a poor quality image (e.g., presence of dark glasses or mouth open). The verification of face image conformance to ISO/ICAO standards is carried out mostly by humans today, through visual inspection, since a totally automatic evaluation is still not satisfactory. The objective of this work is to present the BioLab-ICAO framework, an evaluation benchmark which will be made available to the scientific community, designed to encourage the research on this topic; it consists of a large ground truth database, a well-defined testing protocol, and baseline algorithms for image compliance verification.**

***Index Terms*—E-passports, face image conformance, International Civil Aviation Organization (ICAO), ISO/IEC 19794-5, machine readable travel documents (MRTDs).**

I. Introduction

THE FACE has been traditionally used in identity documents for visual person recognition and, for this reason, it represents one of the most widely accepted characteristics for biometric recognition. With respect to other biometric traits, the face presents several advantages: the acquisition procedure is not intrusive, it does not require the use of expensive hardware, and can be performed even without user cooperation.

Traditional identity documents are now being replaced by electronic documents with biometric features on board; this enables machine-assisted check of person identity, both when the document is issued and successively for identity verification [1], [2] . The International Civil Aviation Organization (ICAO) established a specific working group to determine the most suitable way of "uniquely encoding a particular physical characteristic of a person into a biometric-identifier that can be machine-verified to confirm the presenter's identity" [3]. The decision was taken in 2002 in the so-called "Berlin resolution" which states that: 1) the face is chosen as the primary globally interoperable biometric characteristic for machine-assisted identity confirmation in machine readable travel documents (MRTDs); 2) the Member States have the possibility to use fingerprint and/or iris recognition as additional biometric technologies in support of machine-assisted identity confirmation.

The use of the face as a biometric identifier has some drawbacks: in particular the recognition accuracy is lower with respect to other characteristics (e.g., fingerprint) mainly due to the large intraclass variability of face images. Today, a high accuracy level can only be achieved in supervised/cooperative application scenarios and in the presence of good quality images. For this reason machine-assisted face recognition from identity documents requires quite restrictive quality standards to be fulfilled; in particular, the image should not present any defect that could compromise the subsequent recognition stage. To this aim, the ISO/IEC 19794–5 standard [4], starting from the guidelines initially proposed by ICAO [3], specifies rules for encoding, recording, and transmitting the facial image information and defines scene constraints, photographic properties, and digital image attributes of facial images. The standard has been successively integrated with an amendment [5] describing the conditions for taking photographs and two corrigenda [6] which relax some of the constraints defined in the first version. Moreover an additional document [7] has been recently released, aimed at clarifying the terms and definitions that are useful in the specification, use and testing of face image quality metrics, and to define the purpose, intent, and interpretation of face image quality scores. However, the authors of this document clearly state that performance assessment of quality algorithms and standardization of quality algorithms are outside the scope of the document. The ISO/IEC 19794–5 standard is referred to in the ANSI/NIST-ITL 1–2011 standard [8] as one of the standard profiles for face acquisition.

Overall, the ISO/IEC 19794–5 standard provides quite generic guidelines and several examples of acceptable/unacceptable face images; a clear and unambiguous description of all the requirements is still missing. A survey about the perception of the image quality as defined by the ISO standard was performed within the project Two Dimensional Facial Image Quality (2DFIQ) [9]. In the earlier phase of the project, an analysis of requirements related to facial image quality was performed, leading to the definition of the Achto Qualli method describing the quality conformance requirements to be fulfilled. In a second stage of the project, several experts working in the field were interviewed in order to analyze the perception of the quality requirements defined in the standard and of their relevance in relation to the document issuing process. The quite disappointing results obtained show that even experts operating

Manuscript received October 27, 2011; revised April 16, 2012; accepted April 28, 2012. Date of publication May 09, 2012; date of current version July 09, 2012. The associate editor coordinating the review of this manuscript and approving it for publication was Dr. Patrick J. Flynn. This paper has supplementary downloadable material at http://ieeexplore.ieee.org, provided by the author. The file consists of Appendix A. The material is 1.84 MB in size.

The authors are with the Department of Electronics, Computer Sciences and Systems, University of Bologna, 47521 Cesena (FC), Italy (e-mail: matteo.ferrara@unibo.it; annalisa.franco@unibo.it; dario.maio@unibo.it; davide.maltoni@unibo.it).

Color versions of one or more of the figures in this paper are available online at http://ieeexplore.ieee.org.

Digital Object Identifier 10.1109/TIFS.2012.2198643

in the field have often discordant opinions and uncertainties about how to put into practice the guidelines provided by the standard.

In this state of uncertainty, several vendors of biometric technologies started to produce and distribute SDKs able to automatically verify the compliance of face images to the ISO/ICAO standard, in the attempt of semiautomating the document issuing process. Unfortunately, due to the lack of clear specifications and of an appropriate benchmark, comparing the performance of such systems is not easy.

Our work in this field started from the collaboration established by the Biometric Systems Laboratory (University of Bologna) with CNIPA (the National Center for Computer Science in Public Administration, now named DigitPA) and IPZS (Istituto Poligrafico Zecca dello Stato) aimed to objectively evaluate and compare the performance of some commercial products. The project required the definition of precise and unambiguous requirements, the design of an evaluation framework including a proper image database to be used for testing and, finally, test execution and performance evaluation. The preliminary results of this study have been presented in our previous works [10], [11] where a set of 30 well-defined characteristics, related to geometric (e.g., eye location and distance) and photographic (e.g., focus, contrast) properties of face images has been defined and some preliminary tests have been performed. The framework has been successively significantly extended bringing to the definition of a complete evaluation benchmark (a large database of images, protocols, and baseline algorithms), in line with the recent modifications to the ISO standard [6]. The final framework will be made available to the research community. The purpose of this paper is to describe the extended evaluation framework, to outline the baseline algorithms designed for compliance verification and to compare the results obtained by some commercial SDKs against our own algorithms. To the best of our knowledge, this is the first work in the literature presenting and systematically benchmarking automatic algorithms for all the ISO/ICAO requirements. It is worth noting that, in most of the cases, the baseline algorithms designed are not original approaches (we often used very simple techniques or adapted existing ones); however, we believe that presenting the implemented algorithms and their results on intensive tests gives a clear perception of the level of accuracy reachable by existing techniques, highlights the main open challenges, and represents a useful basis for the development of new and more effective techniques.

The paper is organized as follows: in Section II, the state-of-the-art is discussed. Section III presents the proposed benchmark. Section IV describes the baseline algorithms designed to evaluate the compliance of face images. Section V details the tests carried out and discusses the results obtained, and finally Section VI draws some conclusions.

II. Related Works

Image quality assessment has been extensively studied in the literature for general image processing applications. This work focuses on the evaluation of image quality with respect to ISO/IEC 19794–5. Here the concept of "image quality" partially diverges from its traditional definition: a bad quality image is not necessarily a noisy image; several other factors contribute to the definition of a "bad" image (e.g., presence of dark tinted lenses, eyes closed, or mouth open). Due to the specificity of the requirements defined in the ISO standard, only the literature references that are explicitly related to this aspect will be reviewed in this section.

A few works in the literature proposed a more precise formalization of the ISO/ICAO requirements and described some techniques to evaluate their fulfillment. In [12], 17 image requirements are defined in terms of image format and digital, photographic, and scene characteristics. In addition, the authors report a brief description of a possible approach to verify the degree of compliance to each requirement. The quality scores determined for each requirement are finally fused in a single quality score which, as demonstrated by the experiments carried out, exhibits a positive correlation with human perception of quality. Overall the focus of [12] is on the effects of image quality on the recognition accuracy rather than on the evaluation of the compliance with ISO/ICAO specs. A different set of requirements is proposed in [13] where appropriate evaluation algorithms are described as well. The tests have been carried out on a small internally collected database of 189 images most of which are not compliant to ISO/ICAO specifications. On the basis of the requirements specified in the Achto Qualli method, the authors of [14] proposed a web-based system to calculate quality metrics for digital passport photographs. Twenty-eight requirements organized into three categories (photographic requirements, image requirements, and biometric content) are taken into account, and simple approaches are described to evaluate some of the requirements. The paper does not report an extensive experimentation; only the results on a single example image are discussed.

Several other works, addressing only a few specific requirements, have been presented in the literature. In [15] and [16], the requirements related to closed mouth and open eyes are considered. Two different techniques based on multiclassifier systems are proposed to detect occlusions: the former is based on color space techniques, the latter is more complex and robust and exploits Active Shape Models and PCA to detect occlusions with objects colored similarly to the skin. A small set of requirements, mainly related to geometric characteristics of the face, are considered in [17]. A quality index is assigned to each characteristic; the single scores are then combined to obtain a final quality indicator. The problems related to pose, illumination, and focus are analyzed in [18]; Gabor filters are used to evaluate facial symmetry, thus allowing us to analyze both uneven illumination or improper posture, while DCT is used to measure the image sharpness.

A deep analysis of the literature allows us to draw some conclusions: 1) the requirements for image conformance assessment are not yet well defined and even human experts have uncertainties in the application of the standard; 2) publicly available databases of compliant and noncompliant images are needed to objectively assess and compare the performance of existing commercial products and state-of-the-art techniques; 3) the conformance to some of the requirements is difficult to evaluate automatically and, even if some partial contributions

come from the researchers of the field, many problems are still unsolved.

III. BioLab-ICAO Benchmark

This section describes in detail the BioLab-ICAO benchmark, developed in our laboratory and made available to the scientific community through the website [19]. It consists of: 1) a set of requirements, directly derived from the ISO/ICAO standard; 2) a large database of face images and related ground truth data, produced by human experts with a manual labeling process; 3) a testing protocol for objective performance evaluation and comparison; 4) a set of baseline algorithms internally designed to evaluate the compliance to each defined requirement. More details about each item are provided in the following subsections.

A. Requirements

Starting from the indications provided into the ISO standard [4] and its successive modifications [5], [6] , a set of 30 tests has been defined to evaluate the accuracy of automatic systems for compliance verification (see Table I).

The tests can be organized into three categories:

1) *Feature extraction accuracy*: these tests evaluate the accuracy of eyes and face detection.
2) *Geometric properties of the image*: the tests of this category are aimed to verify if the image fulfills the ISO standard constraints related to the face size and its position within the image. The geometric requirements are specified as a function of some measures represented in Fig. 1.
3) *Photographic and pose-specific tests*: the face must be clearly visible and recognizable; this requirement implies several constraints that generate most of the uncertainties in the interpretation of the ISO standard. A precise formalization is here proposed to limit as much as possible the ambiguity.

B. Database

Evaluating automatic systems aimed to verify the compliance of face images to the ISO standard requires a large database of images representative of many different possible defects (see Table I). The publicly available databases of images only deal with a limited subset of these characteristics (e.g., several face databases contain images affected by illumination problems), but none of them entirely covers the needs of this specific application. For this reason an ad hoc database has been created using, where possible, public databases and acquiring additional images to cover the missing defects. The database contains 5588 images of 601 subjects, gathered from different sources:

- 1741 images from the AR database [20], size 768×576;
- 1935 images from the FRGC database [21], size 1704×2272 or 1200×1600;
- 291 images from the PUT database [22], size 2048×1536;
- 804 images artificially generated by applying ink-marked/creased, pixelation and washed-out effects to compliant images from the AR database;
- 817 newly acquired images of size 1600×1200.

The database consists of 310 fully compliant images (i.e., compliant to all the requirements) and 5278 images not compliant to one or more characteristics (see Figs. A.1 and A.2, respectively).

TABLE I
Tests Defined to Evaluate Systems for ISO/IEC 19794–5 Compliance Check

N°	Description of the test
	Feature extraction accuracy tests
1	Eye Location Accuracy
2	Face Location Accuracy (other points)
	Geometric tests (Full Frontal Image Format)
3	Eye Distance (min 90 pixels)
4	Vertical Position ($0.3B \leq M_y \leq 0.5B$[1])
5	Horizontal Position($0.45A \leq M_x \leq 0.55A$)
6	Head Image Width Ratio ($0.5A \leq CC \leq 0.75A$)
7	Head Image Height Ratio ($0.6B \leq DD \leq 0.9B$[2])
	Photographic and pose-specific tests
8	Blurred
9	Looking Away
10	Ink Marked/Creased
11	Unnatural Skin Tone
12	Too Dark/Light
13	Washed Out
14	Pixelation
15	Hair Across Eyes
16	Eyes Closed
17	Varied Background
18	Roll/Pitch/Yaw Greater than 8°
19	Flash Reflection on Skin
20	Red Eyes
21	Shadows Behind Head
22	Shadows Across Face
23	Dark Tinted Lenses
24	Flash Reflection on Lenses
25	Frames too Heavy
26	Frame Covering Eyes
27	Hat/Cap
28	Veil over Face
29	Mouth Open
30	Presence of Other Faces or Toys too Close to Face

[1] $0.3B \leq M_y \leq 0.6B$ for children under the age of 11 years.
[2] $0.5B \leq DD \leq 0.9B$ for children under the age of 11 years.

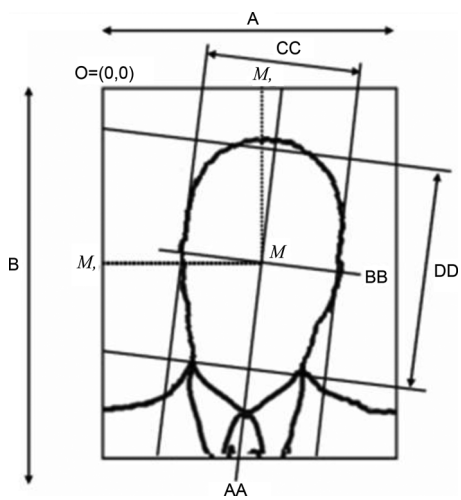

Fig. 1. Geometric characteristics of the full frontal face image format.

TABLE II
COMPOSITION OF THE BIOLAB-ICAO DATABASE (TRAINING SET AND TEST SET). FOR EACH CHARACTERISTIC (8…30), THE NUMBER OF COMPLIANT (C), NONCOMPLIANT (NC), AND DUMMY IMAGES (D) IS REPORTED

N°	Training set			Test set			
	C	NC	D	C	NC	D	n_i
8	661	32	27	4432	317	119	520
9	537	65	118	3439	437	992	520
10	690	30	0	4659	208	1	416
11	523	38	159	3341	567	960	520
12	652	38	30	4367	265	236	520
13	684	34	2	4573	272	23	520
14	690	30	0	4634	233	1	466
15	639	44	37	4326	238	304	476
16	604	31	85	3941	271	656	520
17	395	155	170	2742	1040	1086	520
18	555	51	114	3857	325	686	520
19	569	51	100	3697	400	771	520
20	538	30	152	3586	202	1080	404
21	565	35	120	3774	215	879	430
22	430	147	143	2953	1041	874	520
23	687	31	2	4599	263	6	520
24	621	88	11	4268	516	84	520
25	687	33	0	4650	215	3	430
26	617	33	70	4001	280	587	520
27	687	32	1	4611	257	0	514
28	646	73	1	4494	364	10	520
29	467	126	127	3349	875	644	520
30	671	39	10	4574	222	72	444

The database is supplied with the ground-truth data needed for an objective performance evaluation; in particular the following information is given for each image:

- coordinates of the main facial features (i.e., eye center and corners, nose center, left and right nostrils, mouth corners, and upper and lower lip center);
- compliance to the photographic and pose requirements expressed on the basis of a three-state logic: 1) compliant, 2) noncompliant, and 3) dummy. The dummy value is used for the cases of uncertainty (e.g., when the person wears dark tinted lenses it is not possible to understand if the eyes are open even for human experts).

C. Testing Protocol

The algorithms for compliance verification are usually characterized by a set of parameters that need to be tuned according to the kind of images the algorithm has to process. For this reason, a training set of 720 images (of which 50 are fully compliant) has been extracted from the BioLab-ICAO database to be used for parameters setup and training. The rest of the images are used for testing.

Some information about the composition of both training and test set are given in Table II where for each characteristic the number of compliant, noncompliant, and dummy images are reported. In order to perform balanced tests, the testing set has been further divided into 24 subsets, each related to a specific characteristic.

The subset used to evaluate eye localization accuracy contains all the images where both the pupils centers are visible (3935 images, i.e., all the images in the testing set excluding those with eyes closed and dark tinted lenses); for all the other tests (8–30), the number of images n_i included in the subset related to the characteristic i is: $n_i = 2 \times \min(nc_i, fc)$, where nc_i is the number of images noncompliant to the characteristic i and fc is the number of fully compliant images. Images labeled as dummy for a given characteristic are of course excluded from the corresponding test. The testing protocol adopted requires the SDK to output a compliance degree in the range $[0 \ldots 100]$ for each requirement, where 100 indicates that the image if compliant for that requirement and 0 means it is noncompliant. In some cases, the SDK can fail to process the image or to evaluate a specific characteristic on the image; in these cases a rejection occurs. If the image is processed, the SDK typically compares the degree of compliance with a predefined threshold to decide if the image should be accepted or rejected. Two kinds of error can be made by the software for compliance verification:

1) *False Acceptance*: declaring compliant with respect to a given characteristic an image that is noncompliant;
2) *False Rejection*: declaring noncompliant an image that is compliant.

Starting from the distribution of the degrees of compliance, the equal error rate (EER) is calculated and used to evaluate the performance for each characteristic. The EER is defined as the error rate measured when false acceptance rate equals false rejection rate. According to the best practices, rejections are here implicitly included in the calculation of EER by assuming that a noncompliant result (for the given characteristic) is returned in case of rejection. This choice is aimed at discouraging the software to reject the most uncertain cases thus improving the performance over processed images. It is worth noting that each testing subset is related to a specific characteristic and that consequently only the software response for that characteristic is considered for EER calculation.

IV. BASELINE ALGORITHMS

In this section, our baseline algorithms are described. In some cases, existing algorithms have been appropriately revised and adapted to this specific problem. Due to a lack of space, just a brief description of each algorithm is provided here.

A. Calculation of Basic Image Features

The techniques used for compliance evaluation exploit some basic information extracted from the input image. In particular, the representation of the RGB image in different color spaces is calculated: gray scale (by averaging the RGB channels), HSL [23], $YCbCr$ [24], YUV [25], and XYZ [26]. Moreover, aimed at reducing the effects of illumination, a normalized representation is derived by applying to the input image the automatic color correction proposed by Storer *et al.* in [16].

A crucial step for face image compliance evaluation is the precise localization of face and facial features; most of the subsequent tests, in fact, rely on this information:

- *Face position*: the bounding box enclosing the face of the subject is obtained by a weighted fusion of the results obtained by combining the algorithms proposed by Maio and Maltoni in [27], and Viola and Jones in [28].
- *Eyes position*: starting from the face rectangle, first the coordinates of the centers of the two eye pupils are determined and then the coordinates of the four eye corners are calculated using a variation of the algorithms proposed by

Dobes *et al.* in [29] and by Yuille *et al.* in [30], respectively. If the detection fails due to partial or total coverage of the eyes (e.g., hairs across eyes or dark tinted lenses), the coordinates corresponding to the average position of eye pupils and corners, as measured on the training set, are returned.

- *Nose position*: a rectangular region NR, where the nose is probably located, is preselected according to the face rectangle B and the eye positions. A rigid template matching approach is then applied on the region NR to find out the position of the nose.
- *Mouth position*: the method used to detect the mouth region is a combination of the approaches proposed by Eveno *et al.* in [31] and [32].
- *Presence of glasses*: to assess some requirements (i.e., 23, 24, 25, and 26), it may be very important to know whether the subject in the image wears glasses or not. For this purpose the method proposed by Jing and Mariani in [33] has been used. This method returns a probability $p_{\mathrm{GLASSES}} \in [0;1]$.
- *Face image segmentation*: the precise knowledge of the position and shape of the main components of a face image (i.e., face, hair, clothes, and background regions) is necessary to evaluate its compliance to some requirements (e.g., flash reflection on skin or hair across eyes). For this purpose, our multiclassifier approach [34], based on color and texture information, has been used. Given an input image I, the method returns an image L (with the same dimensions of I) where each pixel is labeled as face, hair, clothes, or background.

B. Photographic and Pose-Specific Tests

The individual algorithms designed to evaluate the degree of compliance to the ICAO requirements (8,…,30) are briefly described in the rest of this section. The requirements are separately evaluated and a compliance score in the range $[0;100]$ is returned for each of them; the failure of one test does not necessarily imply a failure of the other tests on the same image. Because of a lack of space, several images here cited are reported in Appendix A, which is available online as supplementary downloadable material at http://ieeexplore.ieee.org.

1) ICAO 08—Blurred: The blur level of the face region is evaluated by measuring the *top sharpening index* (TSI) that we proposed in [35] and [36]. The compliance score is obtained by linearly rescaling the TSI value in the range $[0;100]$.

2) ICAO 09—Looking Away: The method is based on the assumption that if eye pupils are not in the center of the eyes, the person is looking away. If the image is not frontal (i.e., not compliant to the requirement ICAO 18—Roll/Pitch/Yaw Greater than 8°), it is assumed the subject is looking away and the compliance score returned is 0. Otherwise, the eye corner coordinates are used to estimate the eye center positions and the divergences between the position of each eye pupil with respect to the corresponding eye center are measured: the compliance score is inversely proportional to the distances of the two pupils from the center of the eyes rescaled in $[0;100]$.

3) ICAO 10—Ink Marked/Creased: The analysis of training images suggests that S, Cb, and Cr channels (from HSL and $YCbCr$ color spaces, respectively) are very useful to evaluate the presence of ink marks or creases on the images, particularly in the background area. If the image has nonuniform background (i.e., it is not compliant to ICAO 17), this characteristic is not evaluated because it is not possible to distinguish between ink marks or creases and nonuniform background colors and textures. Otherwise, the compliance score is calculated as

$$\mathrm{ICAO}_{10} = 100 \cdot \left(1 - \frac{\sum_{p \in L_{\mathrm{BG}}} \left(I_S^{\mathrm{Bin}}(p) + I_{Cb-Cr}^{\mathrm{Bin}}(p)\right)}{255 \cdot 2 \cdot |L_{\mathrm{BG}}|}\right) \tag{1}$$

where L_{BG} is the set of pixels labeled as *background* in L, I_S^{Bin} is the binarized *saturation* channel (see Fig. A.3.b), I_{Cb-Cr}^{Bin} is the binarization of the difference between I_{Cb} and I_{Cr} channels (see Fig. A.3.c) and $|L_{\mathrm{BG}}|$ denotes the cardinality of set L_{BG}.

4) ICAO 11—Unnatural Skin Tone: As described by Ahlvers *et al.* in [37], $YCbCr$ color space is well suited to separate the natural skin tone from possible skin color alterations. The compliance score for this characteristic is simply calculated as the percentage of pixels with a natural skin tone in the bounding box B enclosing the face (see Fig. A.4).

5) ICAO 12—Too Dark/Light: To evaluate this requirement, the gray-scale histogram of the image is analyzed. Usually, while the histogram of an image with a normal illumination presents values distributed across the whole gray level range, pixels in histograms of too dark or too light images are condensed in the lower or in the higher part, respectively. Starting from this consideration, let H_B be the gray-scale histogram of the face region B, after discarding 1% of lowest and highest pixels to avoid outliers, two indicators are calculated as follows:

$$i_1 = \frac{\sum_{g=\min}^{\max} (g \cdot H_B(g))}{\sum_{g=\min}^{\max} H_B(g)} \tag{2}$$

$$i_2 = \frac{\max + \min}{2} \tag{3}$$

where $\max$ and $\min$ are the maximum and the minimum gray levels with $H_B(\max) > 0$ and $H_B(\min) > 0$, respectively. The compliance score is calculated as

$$\mathrm{ICAO}_{12} = 100 \cdot \left(1 - \frac{|128 - m|}{128}\right)$$
$$m = \frac{i_1 + i_2}{2} \tag{4}$$

where $|\cdot|$ denotes the absolute value and m is the mean between i_1 and i_2.

6) ICAO 13—Washed Out: Washed out images have a reduced dynamic range (in the gray-scale image) with respect to images with natural colors. The compliance score is simply calculated by rescaling the dynamic range of the gray-scale image to the range $[0;100]$.

7) ICAO 14—Pixelation: The pixelation effect is revealed by the presence of several perfectly horizontal and vertical edges (see Fig. 2). Starting from this simple observation, an ad hoc algorithm has been developed to measure the presence of horizontal and vertical edges. First the gradient modulus, in the eye region, is calculated by using the Prewitt operator [38] and binarized by means of a fixed threshold, then the Hough transform

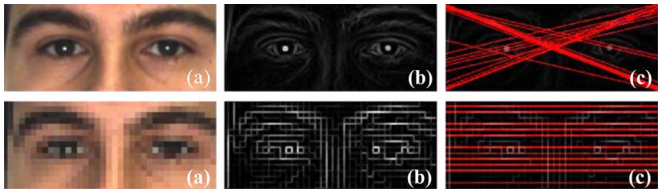

Fig. 2. ICAO 14—Pixelation. The two rows report the results of the algorithm applied to a compliant and a noncompliant image, respectively. In particular, (a) the eye regions, (b) the gradient modulus, and (c) the Hough line detector result are reported.

[39] is used to identify lines on the binarized image. The compliance score is inversely proportional to the number of horizontal and vertical lines found.

8) ICAO 15—Hair Across Eyes: To assess the presence of hair across eyes, an improved version of our approach proposed in [34] is used. The compliance score is inversely proportional to the percentage of pixels in the neighborhoods of the eye positions labeled as *hair* in L (see Fig. A.5).

9) ICAO 16—Eyes Closed: This characteristic is evaluated by measuring the percentage of visible eyes sclera in the subject. The regions that are supposed to contain the eye sclera are identified by using the eye corner and pupil positions; then the number of pixels with an RGB color very similar to the sclera color inside the regions found is determined. The compliance score is calculated as the percentage of pixels, belonging to the considered regions, labeled as sclera.

10) ICAO 17—Varied Background: To assess this requirement, the method proposed in [34], based on the detection of edges in the background area, is used. Given the labeled image L, the gradient modulus of the *saturation* channel of the input image is calculated by using the Prewitt operator [38]; then the compliance score is inversely proportional to the percentage of edge pixels in the background area (see Fig. A.6).

11) ICAO 18—Roll/Pitch/Yaw Greater Than 8°: The algorithm used to evaluate this characteristic is composed by three modules; each of them is able to estimate the rotation of the subject in one of the three dimensions. The first module estimates the *roll* angle by calculating the deviation between the x-axis and the line connecting the two eye pupils. The second module estimates the *pitch* angle by calculating three features: i) distance between the center of the eyes and the tip of the nose; ii) distance between the center of the eyes and the upper bound of the mouth; and iii) distance between the tip of the nose and the upper bound of the mouth. If these distances exceed predefined thresholds the subject presents a *pitch* rotation. The third module estimates the *yaw* rotation is based on the method proposed by Abdel-Mottaleb and Mahoor in [40]. Finally, the results of the three modules are fused using a weighted sum to obtain a compliance score.

12) ICAO 19—Flash Reflection on Skin: The approach proposed in [34] is used to evaluate the compliance to this requirement. Flash reflection on skin is well evident in the image obtained as the difference between the *saturation* and the *red-difference chroma* channels (in HSL and $YCbCr$ color space, respectively). Given the labeled image , the compliance score is inversely proportional to the percentage of pixels with flash reflection in the face region (see Fig. A.7).

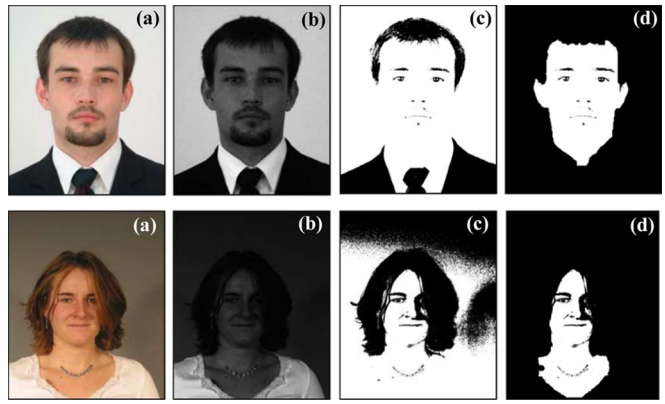

Fig. 3. ICAO 22–Shadows across face. The two rows report the results of the algorithm applied to a compliant and a noncompliant image, respectively. In particular, (a) the input images, (b) the Z channels, (c) the binarized Z channels, and (d) the binarized Z channels in the face region are reported.

13) ICAO 20—Red Eyes: To assess the presence of red eyes, the approach proposed by Zhang *et al.* in [41] is used. The iris regions are identified using the pupil positions then, the color of each pixel, belonging to these regions, is compared to an RGB threshold and classified as natural or red eye color. The compliance score is proportional to the percentage of natural pixels in the iris areas.

14) ICAO 21—Shadows Behind Head: The analysis of training images revealed that the X channel (from the XYZ color space) highlights very well the presence of shadows behind head when the background is uniform. If the image has nonuniform background (i.e., it is not compliant to ICAO 17), this characteristic is not evaluated. Otherwise, the compliance score is inversely proportional to the ratio between the sum of X channel in the background region and the number of background pixels (see Fig. A.8).

15) ICAO 22—Shadows Across Face: The presence of shadows across the face is well evident in the Z channel (from the XYZ color space), as shown in Fig. 3. Given the labeled image L and the binarized Z channel Z_{Bin}, the compliance score is calculated as the percentage of nonzero pixels in Z_{Bin} labeled as *face* in L.

16) ICAO 23—Dark Tinted Lenses: To assess if the subject wears glasses with dark tinted lenses, the probability that the subject in the image wears glasses is combined with a variant to the approach proposed by Storer *et al.* in [16]. Analyzing training images it was noted that the U and V channels (from the YUV color space) highlights better dark tinted lenses than the H channel (originally used in [16]). In particular, let M be a rectangular mask covering the eyes region and I^{Bin}_{U-V} (see Fig. A.9.e) be the binarized image of the difference between U and V channels (see Fig. A.9.c-d, respectively) derived from the color corrected image (see Fig. A.9.b), the compliance score is obtained by the product of p_{GLASSES} (see Section IV-A) and the percentage of nonoccluded pixels (i.e., equal to 0 in I^{Bin}_{U-V}) in the region M.

17) ICAO 24—Flash Reflection on Lenses: The approach to verify this requirement combines the probability p_{GLASSES} that glasses are present in the image with the score of an ad hoc algorithm based on the RBG color segmentation of the eye

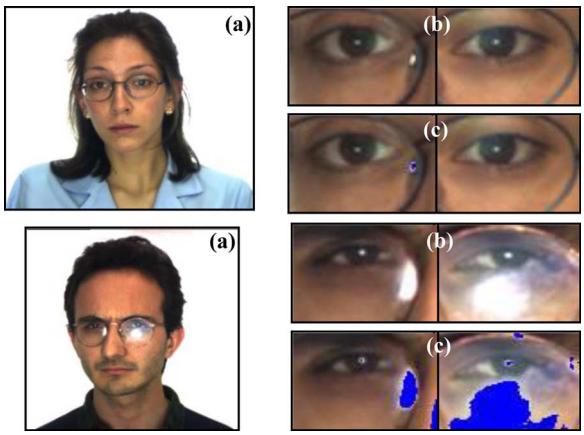

Fig. 4. ICAO 24–Flash reflection on lenses. The images report the results of the algorithm applied to a compliant and a noncompliant image. In particular, (a) the input images, (b) the left and right eye regions, and (c) the eye regions with flash reflection pixels highlighted in blue.

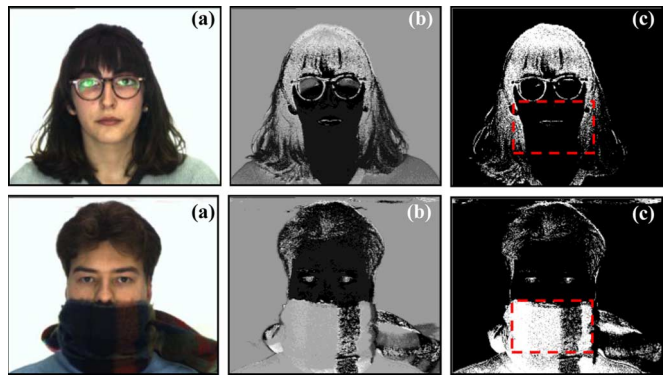

Fig. 5. ICAO 28—Veil over face. The two rows report the results of the algorithm applied to a compliant and a noncompliant image, respectively. In particular, (a) the color corrected images, (b) the H channels, and (c) the binarized H channels and the veil regions considered are shown.

regions. For each pixel contained in these regions, if its color meets the constraints in the RBG color space, it is labeled as flash reflection pixel. The compliance score is calculated as the product of p_{GLASSES} and the percentage of nonflash reflection pixels (see Fig. 4).

18) ICAO 25—Frames Too Heavy: This characteristic is evaluated combining the same method used to evaluate ICAO 11 requirement (i.e., unnatural skin tone) proposed by Ahlvers *et al.* in [37] and the probability that the subject in the image wears glasses. In particular, let M be a rectangular mask covering the eyes region, the compliance score is obtained by the product of p_{GLASSES} and the percentage of pixels with a non-natural skin tone in the region M (see Fig. A.10).

19) ICAO 26—Frames Covering Eyes: The algorithm to evaluate this characteristic combines the probability p_{GLASSES} that glasses are present in the image with the score of an ad hoc method based on the presence of horizontal edges on the eyes. Given I_{LeftEye} and I_{RightEye}, the subimages of the left and right eye, respectively, the vertical derivative approximations of the two images are calculated by using the Prewitt operator [38] and binarized by means of a fixed threshold. Finally, the Hough transform algorithm [39] is used to identify the presence of lines on the two binarized images; the compliance score is calculated as the product of p_{GLASSES} and the percentage of "nonhorizontal" lines.

20) ICAO 27—Hat/Cap: To assess if the subject wears a hat or cap, the approach proposed by Storer *et al.* in [16] is used. Given a rectangular region of the upper part of the face R and the binarized H channel H_{Bin} derived from the color corrected image, the compliance score is proportional to the percentage of nonoccluded pixels (i.e., equal to 0 in H_{Bin}) in the region R (see Fig. A.11).

21) ICAO 28—Veil Over Face: To assess the presence of veil over the face of the subject, the approach proposed by Storer *et al.* in [16] is used. Given a rectangular region of the lower part of the face R and the binarized H channel H_{Bin} derived from the color corrected image, the compliance score is proportional to the percentage of nonoccluded pixels (i.e., equal to 0 in H_{Bin}) in the region R. The main steps of the algorithm are summarized in Fig. 5.

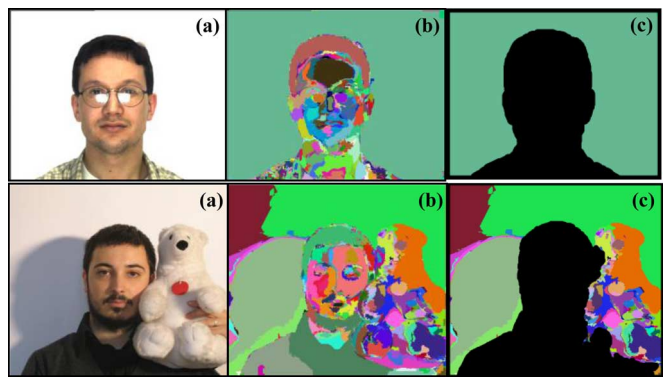

Fig. 6. ICAO 30—Objects close to face. The two rows show the results of the algorithm applied to a compliant and a noncompliant image, respectively. In particular, (a) the input images, (b) the low-level segmentation, and (c) the low-level segmentation in the background regions are reported.

22) ICAO 29—Mouth Open: The size of the mouth region and the presence of teeth are useful features to evaluate this characteristic. The teeth presence is evaluated by simply counting the number of pixels in the mouth region belonging to a predefined region of the RBG color space. The compliance score is calculated by a weighted sum of the mouth height and the teeth presence (see Fig. A.12).

23) ICAO 30—Objects Close to Face: The basic idea to evaluate this requirement is that the presence of objects close to the subject is revealed by regions of different colors in the background area (see Fig. 6). If the image has nonuniform background (i.e., it is not compliant to ICAO 17), this characteristic is not evaluated because it is not possible to distinguish between objects close to the face of the subject and nonuniform background colors and textures. Otherwise, if the background is uniform, the image is partitioned into a set of regions with approximately homogeneous color using the low-level segmentation algorithm based on pyramids implemented in the OpenCV library [42]. Then, given the labeled image L, the compliance score is inversely proportional to the number of regions found in the background area.

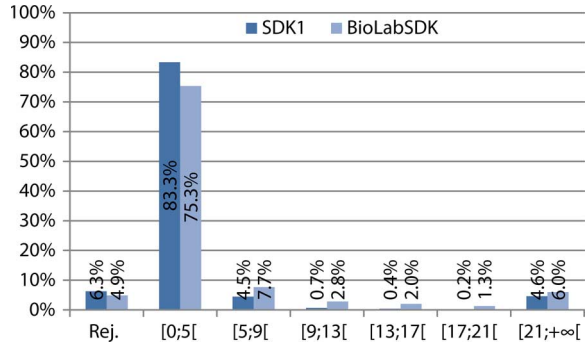

Fig. 7. Eye localization accuracy given as percentage of the total number of images (3935) used in this test. The values defining the intervals are expressed in percentage with respect to the real distance between the two eyes.

V. Experiments

Two commercial SDKs, whose names cannot be disclosed at this stage because of specific agreements with their providers, and the BioLabSDK described in the previous section have been evaluated on the BioLab-ICAO database. The three software will be referred to as SDK1, SDK2, and BioLabSDK, respectively.

The experiments are focused on characteristics 1 (eyes location accuracy) and 8,…,30 (seeTable I); the geometric tests 2,…,7 are not included in this study, because of the nonuniform way the two commercial SDKs provide in output details about the location of internal face features.

As to the geometric requirements, the eye localization accuracy of the SDKs is shown in Fig. 7. The columns refer to increasing intervals of localization errors (percentage value with respect to the real distance between the two eyes). The column "Reject" refers to the images not processed by an SDK. The result for SDK2 is not reported since it does not return the eye position.

In consideration of the peculiarities of the BioLab-ICAO database, which includes images with characteristics that make the eye detection task hard (e.g., presence of hair across eyes or frames too heavy), the performance reached by the two SDKs are satisfactory: the localization error is reasonably small in most cases; in fact, the first interval refers to a very strict constraint (much more restrictive than that used in other works [43]). Moreover, the percentage of rejected images is quite low as well. A deeper performance analysis has been conducted to better understand the main causes of eye detection errors. In particular we selected, overall for the two SDK, the images rejected and those for which the detection error was very high (>20%) and we analyzed their noncompliance to the different requirements (see Fig. 8). Please note that each image can be not compliant to more than one requirement; in this case, it contributes to different characteristics in the histogram. The main causes of detection errors are: subject looking away, varied background, rotated head, presence of shadows, and presence of frames too heavy. The rejections are mainly due to pixelation, hair across eyes, and shadows across face.

In Table III, the results obtained by the three SDKs on tests 8,…,30 are reported, by providing EER and rejection rate for each characteristic.

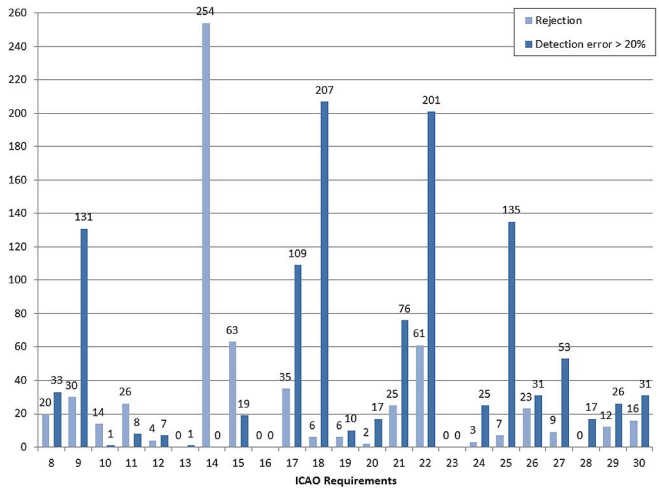

Fig. 8. Images causing a very high eye detection error (>20%) or a rejection are here classified by specific noncompliance. The values reported in the histogram are the sum of the results of SDK1 and BioLabSDK.

TABLE III
EER and Rejection Rate of the Three SDKs Evaluated. The Best Result for Each Characteristic is Bolded

Characteristic	SDK1		SDK2		BioLabSDK	
	EER	Rej.	EER	Rej.	EER	Rej.
8 Blurred	26.0%	8.9%	48.1%	0.6%	**5.2%**	0.0%
9 Looking Away	27.5%	7.1%	-	-	**20.6%**	0.0%
10 Ink Marked/Creased	-	-	-	-	**3.4%**	1.2%
11 Unnatural Skin Tone	18.7%	4.8%	50.0%	0.8%	**4.0%**	0.2%
12 Too Dark/Light	-	-	**3.1%**	0.0%	4.2%	0.0%
13 Washed Out	-	-	40.8%	0.2%	**9.6%**	0.0%
14 Pixelation	-	-	**0.0%**	0.0%	1.3%	0.0%
15 Hair Across Eyes	50.0%	81.9%	-	-	**12.8%**	0.0%
16 Eyes Closed	**2.9%**	3.1%	-	-	4.6%	0.0%
17 Varied Background	7.5%	3.3%	17.9%	1.4%	**5.2%**	0.0%
18 Roll/Pitch/Yaw > 8°	-	-	26.0%	2.9%	**12.7%**	0.2%
19 Flash Refl. on Skin	5.0%	2.7%	50.0%	7.5%	**0.6%**	0.0%
20 Red Eyes	**5.2%**	4.5%	34.2%	0.0%	7.4%	0.0%
21 Shadows Behind Head	-	-	-	-	**2.3%**	0.2%
22 Shadows Across Face	36.4%	8.1%	-	-	**13.1%**	0.4%
23 Dark Tinted Lenses	-	-	-	-	**1.9%**	0.2%
24 Flash Refl. on Lenses	-	-	-	-	**2.1%**	0.0%
25 Frames too Heavy	-	-	-	-	**5.8%**	0.0%
26 Frame Covering Eyes	50.0%	62.3%	-	-	**6.3%**	0.0%
27 Hat/Cap	-	-	-	-	**14.0%**	0.0%
28 Veil over Face	-	-	-	-	**2.5%**	0.0%
29 Mouth Open	**3.3%**	52.1%	-	-	6.2%	0.0%
30 Objects Close to Face	-	-	-	-	**21.6%**	0.0%
- the SDK does not support the test for this characteristic						

The BioLabSDK reaches on the average a good performance (often better than commercial SDKs), even if for some requirements the error rate is still relatively high and further work is needed.

The results of the tests carried out show that there is a great variability in the accuracy of compliance verification and allow us to define three categories of requirements:

1) Some characteristics are relatively *easy* to verify and the SDKs achieve good performance, generally lower than 3%: pixelation, eyes closed, flash reflection on skin, shadows behind head, dark tinted lenses, flash reflection on lenses and veil over face.
2) For others, the evaluated SDKs reach a *medium* accuracy, $3\% \leq \text{EER} \leq 7\%$: blurred, ink marked/creased, unnatural skin tone, too dark/light, varied background, red eyes, frames too heavy, frames covering eyes, and mouth open.

3) The remaining ones are much more *difficult* to evaluate, resulting in EER $> 7\%$ and/or a significant rejection rate: looking away, washed out, hair across eyes, roll/pitch yaw $> 8°$, shadows across face, hat/cap and objects close to face. It is worth noting that for many of this characteristics the poor results are related to the impossibility of correctly detecting the face region (e.g., for excessive head rotation or eyes not clearly visible).

The accuracy obtained on the *easy* requirements suggests that, in this case, a totally automatic verification is feasible with state-of-the-art algorithms. As to the *medium* difficulty requirements, their automatic verification can provide a valid support to human experts; we are confident that further improvements to existing algorithms will allow us to reach a satisfactory accuracy level. Finally for *difficult* requirements, existing algorithms are still not able to adequately assist human experts and significant efforts are needed to find and develop new effective solutions.

VI. Conclusion

In the context of MRTDs, acceptable face images should not present any imperfection that could compromise the recognition process. The traditional indicators are not sufficient to evaluate image quality, and ad hoc algorithms have to be developed to evaluate the requirements described in the ISO/ICAO standards. The BioLab-ICAO framework has been presented in this work with the aim of providing to the scientific community a common benchmark for the evaluation of algorithms for ICAO compliance verification. A large ground-truth database, a precise testing protocol and baseline algorithms for all the ISO/ICAO requirements are made publicly available, thus facilitating further studies on this important topic. According to the results obtained, we can conclude that further improvements are necessary; moreover, the analyzed commercial SDKs only process a subset of the requirements thus confirming that, at this stage, a total automation of image conformance verification is still unfeasible and existing software can only partially support human experts.

As a future work, it would be interesting to study the correlation between ICAO conformance and face recognition accuracy in order to make explicit the impact of the single requirements on recognition performance.

References

[1] T. Bourlai, A. Ross, and A. K. Jain, "On matching digital face images against passport photos," in *Proc. IEEE Int. Conf. Biometrics, Identity and Security*, Tampa, FL, 2009.

[2] T. Bourlai, A. Ross, and A. K. Jain, "Restoring degraded face images for matching faxed or scanned photos," *IEEE Trans. Inf. Forensics Security*, vol. 6, no. 2, pp. 371–384, Jun. 2011.

[3] Biometric Deployment of Machine Readable Travel Documents, ICAO 2003.

[4] ISO International Standard ISO/IEC JTC 1/SC 37 N506, Text of FCD 19794–5, Biometric Data Interchange Formats—Part 5: Face Image Data 2004 [Online]. Available: http://isotc.iso.org.

[5] ISO/IEC 19794–5: 2005/Amd 1:2007, Information Technology—Biometric data Interchange format—Part 5: Face Image Data/Amendment 1: Conditions for Taking Photographs for Face Image Data 2007.

[6] ISO/IEC 19794–5: 2005/Cor 1&2:2008, Information Technology—Biometric Data Interchange Format—Part 5: Face Image Data, 2008, Technical Corrigendum 1&2.

[7] ISO/IEC TR 29794-5:2010, Information Technology—Biometric Sample Quality—Part 5: Face Image Data 2010.

[8] ANSI/NIST-ITL 1–2011, Data Format for the Interchange of Fingerprint, Facial & Other Biometric Information 2011.

[9] O. Yuridia and G. Castillo, Survey About Facial Image Quality," Fraunhofer Institute for Computer Graphics Research 2006.

[10] M. Ferrara, M. Franco, and D. Maltoni, "Evaluating systems assessing face-image compliance with ICAO/ISO standards," in *Proc. Eur. Workshop on Biometrics and Identity Management (BIOID 2008)*, Roskilde, Denmark, 2008, pp. 191–199.

[11] D. Maltoni, A. Franco, M. Ferrara, D. Maio, and A. Nardelli, "Biolab-ICAO: A new Bench4–5 standard," in *Proc. 16th Int. Conf. Image Processing (2009)*, 2009, pp. 41–44.

[12] R. L. V. Hsu, J. Shah, and B. Martin, "Quality assessment of facial images," in *Proc. Biometric Consortium Conf.*, 2006, pp. 1–6.

[13] M. Subasic, S. Loncaric, T. Petkovic, H. Bogunovic, and V. Krivec, "Face image validation system," in *Proc. Int. Symp. Image and Signal Processing and Analysis (2005)*, 2005, pp. 30–33.

[14] O. Y. Gonzalez-Castillo and K. Delac, "A web based system to calculate quality metrics for digital passport photographs," in *Proc. 8th Mexican Int. Conf. Current Trends in Computer Science*, 2007, pp. 105–112.

[15] M. Storer, M. Urschler, H. Bischof, and J. A. Birchbauer, "Classifier fusion for robust ICAO compliant face analysis," in *Proc. IEEE Int. Conf. Automatic Face and Gesture Recognition*, 2008, pp. 1–8.

[16] M. Storer, M. Urschler, and H. Bischof, "Occlusion detection for ICAO compliant facial photographs," in *Proc. IEEE Conf. Computer Vision and Pattern Recognition (CVPR), Workshop on Biometrics*, 2010, pp. 122–129.

[17] Q. Han, Y. Gonzalez, J. M. Guerrero, and X. Niu, "Evaluating the content-related quality of digital ID images," in *Proc. Congress on Image and Signal Processing*, 2008, pp. 440–444.

[18] J. Sang, Z. Lei, S. Z. Li, J. Sang, Z. L. Stan, and Z. Li, "Face image quality evaluation for ISO/IEC standards 19794–5 and 29794–5," in *Proc. Int. Conf. Biometrics*, 2009, pp. 229–238.

[19] BioLab. Biometric System Laboratory web site Apr. 2012 [Online]. Available: http://biolab.csr.unibo.it

[20] A. M. Martinez and R. Benavente, The AR Face Database, CVC Computer Vision Center, 1998.

[21] P. J. Phillips *et al.*, "Overview of the face recognition grand challenge," in *Proc. IEEE Computer Vision and Pattern Recognition*, 2005, vol. 1, pp. 947–954.

[22] A. Kasinnski, A. Florek, and A. Schmidt, "The PUT face database," *Image Process. Commun.*, vol. 13, no. 3–4, pp. 59–64, 2008.

[23] Wikipedia. HSL color space Sep. 2011 [Online]. Available: http://en.wikipedia.org/wiki/HSL_color_space

[24] Wikipedia. YCbCr color space Apr. 2012 [Online]. Available: http://en.wikipedia.org/wiki/YCbCr

[25] Wikipedia. YUV Color Space Apr. 2012 [Online]. Available: http://en.wikipedia.org/wiki/YUV

[26] Wikipedia. XYZ Color Space Apr. 2012 [Online]. Available: http://en.wikipedia.org/wiki/CIE_1931_color_space

[27] D. Maio and D. Maltoni, "Real-time face location on gray-scale static images," *Pattern Recognit.*, vol. 33, no. 9, pp. 1525–1539, 2000.

[28] P. Viola and M. Jones, "Rapid object detection using a boosted cascade of simple features," in *Proc. IEEE Int. Conf. Computer Vision and Pattern Recognition*, 2001, vol. 1, pp. 511–518.

[29] M. Dobes *et al.*, "Human eye localization using the modified Hough transform," *Optik—Int. J. Light Electron Opt.*, vol. 117, no. 10, pp. 468–473, Oct. 2006.

[30] A. L. Yuille, P. W. Hallinan, and D. S. Cohen, "Feature extraction from faces using deformable templates," *Int. J. Comput. Vis.*, vol. 8, no. 2, pp. 99–111, 1992.

[31] N. Eveno, A. Caplier, and P. Y. Coulon, "A new color transformation for lips segmentation," in *Proc. IEEE Fourth Workshop on Multimedia Signal Processing*, 2001, pp. 3–8.

[32] N. Eveno, A. Caplier, and P. Y. Coulon, "Key points based segmentation of lips," in *Proc. IEEE Int. Conf. Multimedia and Expo*, Lausanne, Switzerland, 2002.

[33] Z. Jing and R. Mariani, "Glasses detection and extraction by deformable contour," in *Proc. 15th Int. Conf. Pattern Recognition (ICPR'00)*, 2000, vol. 2, pp. 933–936.

[34] M. Ferrara, A. Franco, and D. Maio, "A multi-classifier approach to face image segmentation for travel documents," *Expert Systems with Applications*, vol. 39, no. 9, pp. 8452–8466, Jul. 2012.

[35] M. Ferrara, A. Franco, and D. Maltoni, "Estimating image focusing in fingerprint scanners," in *Proc. Workshop on Automatic Identification Advances Technologies (AutoID07)*, Alghero, Italy, 2007, pp. 30–34.

[36] M. Ferrara, A. Franco, and D. Maltoni, "Fingerprint scanner focusing estimation by top sharpening index," in *Proc. 14th Int. Conf. Image Analysis and Processing (ICIAP07)*, Modena, Italy, 2007, pp. 223–228.
[37] U. Ahlvers, U. Zölzer, and R. Rajagopalan, "Model-free face detection and head tracking with morphological hole mapping," in *Proc. 13th Eur. Signal Processing Conf. (EUSIPCO'05)*, Antalya, Turkey, 2005.
[38] R. C. Gonzalez and R. E. Woods*, Digital Image Processing*, 2nd ed. Boston, MA: Addison-Wesley Longman Publishing Co., Inc, 1992.
[39] R. O. Duda and P. E. Hart, "Use of the Hough transformation to detect lines and curves in pictures," *Commun. ACM*, vol. 15, no. 1, pp. 11–15, Jan. 1972.
[40] M. Abdel-Mottaleb and M. H. Mahoor, "Algorithms for assessing the quality of facial images," *IEEE Computat. Intell. Mag.*, vol. 2, no. 2, pp. 10–17, May 2007.
[41] L. Zhang, Y. Sun, M. Li, and H. Zhang, "Automated red-eye detection and correction in digital photographs," in *Proc. Int. Conf. Image Processing (ICIP '04)*, 2004, vol. 4, pp. 2363–2366.
[42] OpenCV. OpenCV Library Apr. 2012 [Online]. Available: http://opencv.willowgarage.com/wiki/
[43] T. Bourlai, C. Whitelam, and I. Kakadiaris, "Pupil detection under lighting and pose variations in the visible and active infrared bands," in *Proc. IEEE Int. Workshop on Information Forensics and Security*, 2011, pp. 1–6.

Matteo Ferrara received the bachelor's degree *cum laude* in computer science from the University of Bologna, in March 2004, and the Master's degree *cum laude* in October 2005. He received the Ph.D. degree from the Department of Electronics, Computer Science and Systems (DEIS), University of Bologna.

During his Ph.D. studies, which he completed in 2009, he worked on Biometric Fingerprint Recognition Systems. Today he is an assistant teacher in Computer Architectures and Pattern Recognition courses at the faculty of Computer Science, University of Bologna, and he is a member of the Biometric System Laboratory, Cesena, Italy. His research interests include image processing, pattern recognition, biometric systems (fingerprint recognition, performance evaluation of biometric systems, fingerprint scanner quality, and face recognition), information security, and smart card.

Annalisa Franco received the Laurea degree *cum laude* in computer science in 2000 from the University of Bologna. In 2004, she received the Ph.D. degree in electronics, computer science and telecommunications engineering at Department of Electronics, Informatics and Systems (DEIS), University of Bologna, for her work on multidimensional indexing structures and their application as pattern recognition.

She is a Researcher at the DEIS, University of Bologna. She teaches "Biometric Systems" at Computer Science, University of Bologna, and she is member of the Biometric Systems Laboratory, Cesena, Italy. Her research interests include pattern recognition, biometric systems (in particular face detection and recognition, fingerprint recognition), image databases (content-based image retrieval, relevance feedback), and multidimensional data structures.

Dario Maio (M'90) received a degree in Electronic Engineering from the University of Bologna in 1975.

He is a Full Professor at the University of Bologna. He is director of the Biometric Systems Laboratory, Cesena, Italy. He has published over 190 papers in numerous fields, including distributed computer systems, computer performance evaluation, database design, information systems, neural networks, autonomous agents, and biometric systems. He is author of the book, *Biometric Systems, Technology, Design and Performance Evaluation*, Springer 2005, and of the *Handbook of Fingerprint Recognition*, Springer 2003, II edition 2009. He is with DEIS and IEIIT-C.N.R.; he teaches database systems and biometric systems.

Davide Maltoni (M'05) is an Associate Professor at the Department of Electronics, Informatics and Systems (DEIS), University of Bologna. He teaches "Computer Architectures" and "Pattern Recognition" at Computer Science, University of Bologna, Cesena. His research interests are in the area of pattern recognition and computer vision. He is active in the field of biometric systems (fingerprint recognition, face recognition, hand recognition, performance evaluation of biometric systems). He is codirector of the Biometric Systems Laboratory, Cesena, Italy, which is internationally known for its research and publications in the field. He is author of two books, *Biometric Systems, Technology, Design and Performance Evaluation*, Springer 2005, and *Handbook of Fingerprint Recognition*, Springer 2003, II edition 2009, which received the PSP award from the Association of American Publishers.